The ground-state phase diagram of the two-dimensional Falicov-Kimball model

1995 J. Phys.: Condens. Matter 7 9521

(http://iopscience.iop.org/0953-8984/7/49/016)

J. Phys.: Condens. Matter 7 (1995) 9521–9542. Printed in the UK

The ground-state phase diagram of the two-dimensional Falicov–Kimball model

G I Watson†§ and R Lemanski‡‖

† Rutherford Appleton Laboratory, Oxfordshire OX11 0QX, UK
‡ Institute for Low Temperature and Structure Research, Polish Academy of Sciences, PO Box 937, 50-950 Wrocław 2, Poland

Received 22 May 1995, in final form 29 August 1995

Abstract. The spinless Falicov–Kimball model on a two-dimensional square lattice is studied using the method of restricted phase diagrams constructed in the grand canonical ensemble. The results are compared with the one-dimensional model. Although the two-dimensional phase diagrams are more complex, with several distinct families of ion configurations occurring as ground states, there are surprising similarities with the one-dimensional case. Within each family of configurations, the ground states form a devil's staircase structure and the configurations are constructed according to a composition rule identical to that in one dimension. It is also found that, as in one dimension, segregation occurs in the non-neutral model for large ion–electron interaction strength. Some features of the phase diagrams are understood by examining the effective two-body ion interaction.

1. Introduction

There are several reasons for the continued interest in the Falicov–Kimball model (FKM) over the past several decades. The model was originally proposed [1] as a model of metal–insulator transitions in mixed-valence compounds of rare earths and transition metals. Since then, it has been studied as a model of crystallization due to effective interactions mediated by band electrons, as a variant of the Hubbard model [2], and as a model of binary alloys [3]. Our interest is motivated by the fact that the FKM is the simplest known model with nontrivial many-body correlation effects. It is amenable to analytical treatment and controlled approximations, and the solutions typically show a form of charge-density-wave order in the ground state. Therefore, we view the FKM as a tool for studying the tendency for charge-density-wave formation in more general interacting fermion systems, as well as a model of physical interest in its own right. Work on applying results from the FKM to more general contexts includes the construction of a strong-coupling mean-field theory of the Hubbard model [3, 4], an investigation of the breakdown of Fermi liquid theory [5], a study of electron–phonon interactions [6], and a study of the asymmetric Hubbard model [7].

In this paper we study the ground-state phase diagram of the spinless FKM on a two-dimensional square lattice. Our study is based on the restricted phase diagrams constructed in the grand canonical ensemble for various values of interaction constant U.

§ E-mail address: giw@isise.rl.ac.uk.
‖ Formerly R Łyżwa.

0953-8984/95/499521+22$19.50

Previous work on the Falicov–Kimball model has concentrated on the one-dimensional case, and there the phase diagram has been found to have a very rich structure [3, 8–10]. In particular, in the limit of large values of U only domains of the so-called most homogeneous configurations of the ions appear in the phase diagram constructed in the grand canonical ensemble [9, 11, 12]. The effective interactions between ions are repulsive in this case. On the other hand, for small values of U, other periodic phases appear in the phase diagram as well as the most homogeneous configurations. If, additionally, the density of the ions is close to zero (or unity) then the formation of molecules containing two or more ions (or vacancies) is observed [9, 10].

Much less is known about the two-dimensional system. It has been proven rigorously [2, 13] that the ground state at half filling ($\rho_i = \rho_e = 1/2$) is the 'chequerboard' configuration (figure 3) and that the long-range order persists to nonzero temperature; this is a general result for bipartite lattices in any dimension greater than one. In [14] the method of restricted phase diagrams was applied to the two-dimensional square lattice, but only configurations with ion density equal to 1/2 were taken into account. Later, some general properties of the phase diagrams were established, and rigorous results were obtained in the limit of large values of U [15–17]. In particular the ground-state configurations of the ions were found for the neutral case ($\rho_i = \rho_e$) and $\rho = 1/3$, $1/4$ and $1/5$, and a characterization of the ground states for densities in the range $1/4 < \rho < 1/2$ was given. In addition, an argument has been proposed [8, 18] suggesting that the phase diagram in the canonical ensemble for the two-dimensional case should be qualitatively the same as that for the $d = \infty$ model, which has been solved exactly [19].

The two-dimensional FKM is much more difficult to study than the one-dimensional one because the analytical formulae for the total energy of a one-dimensional system do not generalize to two dimensions, except for a few special classes of configurations. Thus the total energy of the system for an arbitrary configuration can be found only from direct numerical diagonalization of the Hamiltonian. Another complication is that a much larger set of ionic configurations has to be taken into account to construct a reliable phase diagram.

In the next section we calculate the effective interaction between two ions mediated by itinerant electrons. We also review some rigorous results on the two-dimensional model which provide a skeleton phase diagram, and discuss the solution of the model for periodic ion configurations, on which our numerical work is based. In section 3 we supply some computational details, followed by the results in the form of restricted phase diagrams for various values of the interaction strength U. Section 4 contains discussion of the results and our conclusions.

2. Analytical results

2.1. The model

The spinless Falicov–Kimball model describes the interaction of two species of particle: a set of spinless fermions, conventionally termed electrons and represented by fermion operators $a_i^\dagger$ and a_i on lattice site i, and a set of infinitely massive classical particles, termed ions, described by classical occupation variables w_i taking the values 0 or 1 on each site. In other words, $w_i = 1$ if site i is occupied by an ion, and $w_i = 0$ if site i is vacant. Each particle does not interact with particles of the same species, but there is an on-site interaction between electrons and ions, whose strength is given by the dimensionless

constant U. Thus we write the Hamiltonian

$$H = -\sum_{\langle ij \rangle} a_i^\dagger a_j - U \sum_i w_i n_i - N(\mu_e - U/2)\rho_e - N(\mu_i - U/2)\rho_i \qquad (1)$$

where (ij) means that sites i and j are nearest neighbours, $n_i = a_i^\dagger a_i$ is the electron occupation of site i, N is the number of lattice sites, and $\rho_e = N_e/N$ and $\rho_i = N_i/N$ are electron and ion densities, respectively. The energy scale has been chosen to be the electron bandwidth, so that the electron hopping rate is unity; then U is the energy of the electron–ion interaction in these units. The last two terms are included when we are working in the grand canonical ensemble, and then μ_e and μ_i are the chemical potentials. The independent parameters in the model are U, ρ_e, ρ_i in the canonical ensemble and U, μ_e, μ_i in the grand canonical ensemble.

The problem of constructing the ground-state phase diagram in the grand canonical ensemble is formulated as follows. For a given point (μ_e, μ_i) in the plane of chemical potentials, consider all possible ionic configurations, given by all possible values of the variables w_i. For each configuration, the electron Hamiltonian H_e is given by the first two terms of (1) and represents free electrons moving in a fixed potential created by the ions; the resulting single-particle states of H_e are filled up to the Fermi level E_F, and the total electronic energy $E_T(w, E_F)$ is then to be minimized over all ion configurations and over the Fermi level.

The E_F minimization is trivial and gives, of course,

$$E_F = \mu_e - U/2. \qquad (2)$$

The subsequent minimization over the ion configurations is the nontrivial aspect, and leads to a form of many-body behaviour.

The chemical potentials have been chosen so that the Hamiltonian is invariant (up to a constant) under a transformation consisting of particle–hole inversion of both electrons and ions, followed by $\mu \to -\mu$. It follows that the phase diagram of the model is symmetric with respect to inversion about the origin, in the sense that the ground-state phases at (μ_e, μ_i) and $(-\mu_e, -\mu_i)$ are related by a particle–hole transformation.

Performing a particle–hole transformation on the ions only yields an equivalent Hamiltonian but with $U \to -U$ and $\mu_i \to -\mu_i$. In other words, the attractive and repulsive models transform into one another. Hence it is sufficient to consider a single sign of U; we choose the attractive case, $U > 0$. Physically, one imagines the electrons and ions as having equal and opposite charges, and therefore the case $\rho_e = \rho_i$ is referred to as *neutral*.

2.2. *The effective interaction*

A feature of the FKM is the division into 'fast' quantum mechanical degrees of freedom and 'slow' classical ones, and it is natural to imagine 'integrating out' the electrons, leaving only ions interacting through effective classical potentials [2]. Here we calculate these effective potentials for the case of two ions in an infinite lattice. The calculation is restricted to neutral systems, since this type of analysis has been found to be useful for the one-dimensional model [10, 12].

The use of an effective two-body interaction derived from isolated ions in an infinite empty lattice neglects the influence of other nearby ions on the pair potential of the two ions in question, that is, it neglects three-body and higher-order potentials. Nevertheless, this approach yields important qualitative information. An immediate example is that the

effective potentials may be divided into repulsive and attractive behaviour. In the former case, the ground state would be expected to be homogeneous in the distribution of ions, while in the latter, one would expect the ions to clump together, which is the phenomenon of segregation [3]. For the one-dimensional model, the boundary between the two regimes defines a metal–insulator transition [10], and Lemberger [11] has shown that in the large U limit the homogeneous and segregated configurations exhaust the possibilities for the ground state.

The electron motion in the presence of one or more ions may be thought of as a defect or impurity problem. The electron Hamiltonian is written $H_e = T + V$, where T is the kinetic energy and V is the potential of the ions. If V is attractive, its effect on the energy spectrum of T, if any, is to create one or more bound states, while the extended electron states in the band of T are not perturbed in energy by the ions (in the limit of an infinite system). For two ions at sites 0 and r, the bound state energies are solutions of the implicit equation [20]

$$G_0 \pm G_r = -1/U \tag{3}$$

where $G_r = \langle 0|(E - T)^{-1}|r\rangle$ are matrix elements of the lattice Green function, and U is the strength of the (attractive) defects. Hence there may be zero, one or two bound levels depending on U, the ion separation r, and the dimension of the lattice.

In one dimension, below the band,

$$G_r(E) = -(2\sinh\alpha)^{-1}\mathrm{e}^{-\alpha|r|} \tag{4}$$

where $E = -2\cosh\alpha$, and thus G_r has an inverse square root divergence at the band edge. Also, $G_r - G_0$ tends to the limit $|r|/2$ at the band edge, and we find that there is a critical value, $U_c = 2/|r|$, such that strong attraction ($U > U_c$) gives two bound states and weak attraction ($U < U_c$) only one. The value of U_c decreases with increasing distance between ions, and for nearest-neighbour sites $U_c = 2$, so if $U > 2$ there are always two bound states.

In two dimensions, there is no longer a simple expression for G_r in terms of special functions (although specific cases can be written in terms of complete elliptic integrals). However, the behaviour is qualitatively the same as in the one-dimensional case, with a critical U below which there is only one bound state. For $U > 4$, there are always two bound states.

If two electrons are now added to make a neutral system, these will occupy the lowest two electronic states. Hence we define the total electronic energy, identified as the effective ion interaction, as the sum of the bound-state energies if there are two bound states, and as $E_b - 4$ if there is one bound state. (In the latter case, the second electron occupies a state at the bottom of the band.)

For the two-dimensional problem the effective potential depends on the two-dimensional vector r, but we have found that in most cases the angular dependence is very weak, so the potential has approximate circular symmetry. Deviations from circular symmetry occur due to the discreteness of the lattice, when the length scale of variations in the effective potential matches the lattice spacing. This occurs only near $U = 3.5$, and does not affect the general picture. Therefore, in figure 1, we display results for the effective ion potential $V_{eff}(r)$ with r lying along a lattice axis, for various U. The energy origin is chosen such that $V_{eff}(\infty) = 0$.

The effective potential may be described as having three kinds of qualitative behaviour as U varies. For $U > U_{c2} \approx 3.47$, the potential is purely repulsive, in the sense that the ions may always lower their energy by moving away from one another. In an intermediate range, $U_{c1} < U < U_{c2}$, with $U_{c1} = 3.26$, the potential is repulsive in the sense that it is minimized

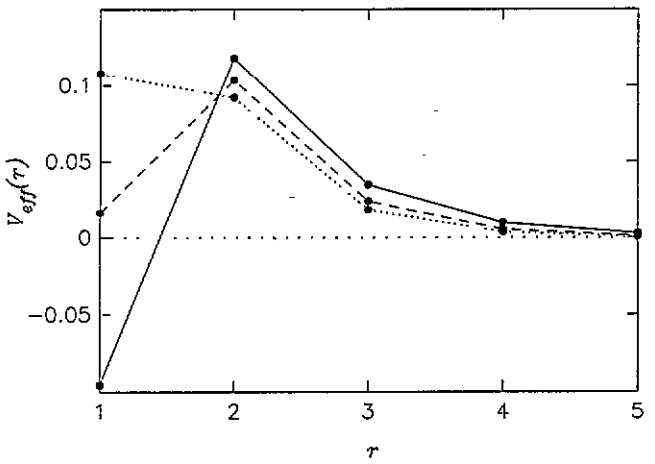

Figure 1. The effective pair potential of two classical ions, mediated by two mobile electrons in a infinite two-dimensional square lattice, plotted as a function of the ion separation r along a lattice axis. The data points are joined by lines as a guide to the eye. Three values of the ion–electron interaction constant U are used: continuous line, $U = 3$; dashed line, $U = 3.3$; dotted line, $U = 3.5$.

for infinite separation, but there is a short-range attractive part which may result in the trapping of the ion. Finally, for $U < U_{c1}$, the potential remains attractive when the ions are near each other and repulsive when they are far apart, but the dominant behaviour is now attractive since the global energy minimum occurs when the ions are nearest neighbours.

These results are very similar to the one-dimensional case [10], except that there the critical values are $U_{c1} = 2/\sqrt{3} \approx 1.15$ and $U_{c2} \approx 1.61$.

The essential features of the effective potentials may be understood by the following simple argument. When the ions are well separated, the electrons reside in the approximate single-ion bound levels, i.e. each ion traps one electron to form an atom. The long-range interaction is therefore repulsive, because Pauli exclusion resists the overlapping of electron wavefunctions that occurs when the atoms are brought together. Using a variational wavefunction constructed from single-defect states, it is easy to show that this repulsive tail of the effective potential is proportional to $re^{-\alpha r}$. Conversely, when the ions are sufficiently close together, only one electron is trapped in a 'molecular' bound level, and the other electron is delocalized. Here, the energy is reduced by bringing the ions closer together in order to bind the former electron more strongly. Therefore, if the ions were moving in a continuum, the effective potential would always be attractive at short range [12, 21]. However, the range of the attractive part decreases rapidly with increasing U as the wavefunctions become more tightly bound, and since on a lattice the ions cannot approach closer than nearest-neighbour sites, one finds a completely repulsive regime for large U.

On the basis of these results we may make some predictions concerning the appearance of neutral phases in the ground-state phase diagram. When U is greater than about U_{c1}, we would expect the repulsive interaction to give rise to neutral phases with the ions distributed homogeneously in the lattice. For smaller U, it is possible that the ions would come together to form nearest-neighbour pairs, i.e. molecules. The fate of these molecules would then depend on the effective inter-molecular forces: the molecules may adopt a homogeneous distribution, or may come together to form larger aggregates; if the interactions between

aggregates of any size are attractive, segregation would occur. This picture is similar to that found for the one-dimensional model [10].

Another important trend in the form of V_{eff} is the widening of the potential well as U decreases. A consequence is that for small U the effective potential depends relatively weakly on the ion separation within the well: for instance, the difference in energy between the nearest-neighbour and second-nearest-neighbour ions may be slight compared with the energy scale of the depth of the well. This accords with the observation (section 3) that the phase diagram becomes increasingly complicated as U decreases, as small changes in the parameters are capable of altering the energy balance between a large number of nearly degenerate configurations.

These trends predicted by considering the effective ion-pair potentials are generally borne out by the numerical data (see section 3). However, as indicated, the present analysis is a fairly crude tool in understanding the behaviour of the model, and rather than attempting to refine it, we move on to other approaches.

2.3. The skeleton phase diagram

In an elegant analysis, Gruber, Jędrzejewski and Lemberger [16] have derived a number of exact bounds which provide a global picture of the phase diagram of the FKM for a cubic lattice in any dimension. The analysis considers three specific configurations: the full configuration, in which every site is occupied by an ion, the empty configuration, in which every site is vacant, and the chequerboard configuration, in which one sublattice is full and the other is empty.

Their results are summarized schematically in figure 2, for the two-dimensional case with $U < 8$. The diagram is divided into three principal regions. In the upper right region, the ground-state ion configuration is full; in the lower left, it is empty. The exact analysis does not describe the structure of the central region, which we denote $\tilde{\mathcal{D}}$, except to say that there is a domain containing the point $\mu_i = \mu_e = 0$ in which the chequerboard configuration is the ground state.

In the one-dimensional case, the central region $\tilde{\mathcal{D}}$ has been found to contain a very complex structure [9, 10]. In addition to the chequerboard configuration, a wealth of other periodic configurations are ground states in certain regions of the diagram. In fact, it is believed that configurations of arbitrary period occur in domains arranged to form a fractal structure, and that the dependence of ion density on chemical potential is a devil's staircase [3, 9, 10, 22]. If a similar structure occurs in the two-dimensional model, then, it must be confined to $\tilde{\mathcal{D}}$.

Another question concerns the behaviour near the upper left tip of the region $\tilde{\mathcal{D}}$. The horizontal line extending to the left separates empty and full ground states having electron densities equal to zero (in which case all ion configurations are degenerate). For the one-dimensional model, it is found [9] that this line continues inside $\tilde{\mathcal{D}}$, separating full and empty configurations with nonzero electron density, and therefore on the coexistence line itself the ground state may be an incoherent mixture of full and empty configurations, which is termed the segregated phase [3]. The structure of the phase diagram near the tip, therefore, is connected with the phenomenon of segregation. On physical grounds, segregation is expected to be a general phenomenon, but to our knowledge there are no general results on this question in more than one dimension.

The appearance of the phase diagram is somewhat different for $U > 8$. In this case, it can be shown [2] that for any ion configuration the electronic spectrum has a gap containing the interval $[4-U, -4]$, which we term the *principal gap*. Then in the strip $|\mu_e| < U/2-4$

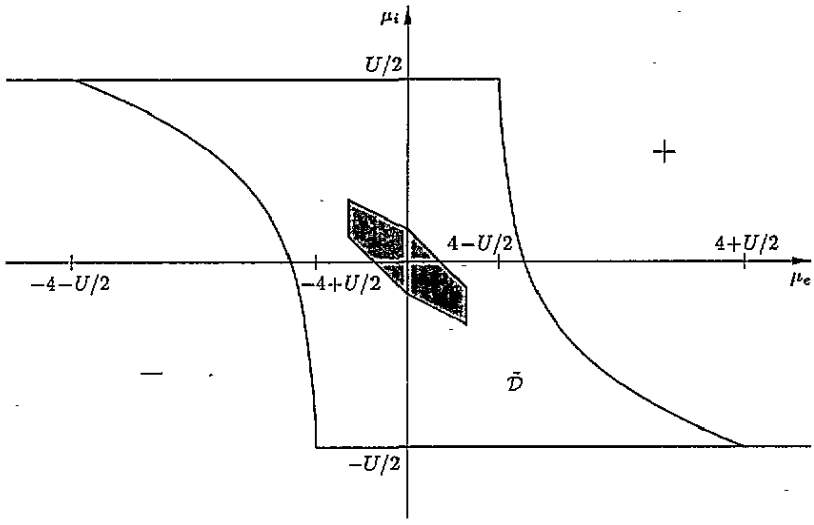

Figure 2. Schematic phase diagram obtained by Gruber *et al* [16]. Lines divide the plane of electron (μ_e) and ion (μ_i) chemical potentials into regions (+) and (−) in which the full and empty configurations, respectively, have been proved to be the ground states, and $\bar{\mathcal{D}}$, in which any translationally non-invariant ground states must be contained. $\bar{\mathcal{D}}$ includes the shaded domain, in which the chequerboard configuration has been shown to be the ground state.

all the ground states are neutral, and have the Fermi energy lying in the principal gap, so the transport properties of the system will be those of an insulator; the phase boundaries here are straight lines inclined at 45°. It is expected that, as in one dimension, the occurrence of insulating neutral phases will begin somewhat below the rigorous bound, $U = 8$.

We now turn to results obtained by Kennedy [17] using rigorous perturbation theory for large U. This work investigated the neutral phases, which in the one-dimensional problem for large U are known to have as ground states the most homogeneous configurations (in a technical sense as defined in [11]). Kennedy determined the ground states for ion (and electron) density $\rho_i = 1/5$, $1/4$ and $1/3$, and proved that for $1/4 \leqslant \rho_i \leqslant 1/2$ the ground states have a one-dimensional character, as described below. The results confirmed the predictions of previous investigations [14, 15], but showed, somewhat surprisingly, that the large-U ground states are not the most homogeneous configurations in any reasonable sense.

The configurations shown by Kennedy to be neutral ground states for large U are shown in figure 3, for $\rho_i = 1/2$ (the chequerboard [2]), $1/3$, $1/4$ and $1/5$. Each of these configurations consists of parallel lines of occupied sites, with all other sites empty. For instance in the density-$1/5$ structure one may draw lines of slope $1/2$ such that every intersection of the line with the lattice is an occupied site, and all occupied sites lie on such a line. Each structure can be described by such lines in more than one way. However, the $\rho = 1/4$ and $\rho = 1/3$ structures have a common description: they both consist of equally spaced lines of occupied sites of slope $1/2$, but differ in the spacing of the lines. Then the following result [17] holds for the density range $1/4 \leqslant \rho \leqslant 1/3$: all the ground-state ion configurations may be described by lines of slope $1/2$ (but their spacing may not be uniform). We denote the structure of the density-$1/4$ state by (1000), which means that it is a periodic repetition of one occupied line followed by three unoccupied lines; the density-$1/3$ state is then (100), and at all intermediate ρ the ground state is given by a binary sequence of appropriate density. A similar result [17] exists for $1/3 \leqslant \rho \leqslant 1/2$, stating

that the ground states consist of parallel lines of slope 1, ranging from (100) at $\rho = 1/3$ to (10) at $\rho = 1/2$.

These ground states, then, have essentially a *one-dimensional* character. Let us define the *characteristic configuration*, C_n, as the neutral ground state of density $1/n$ as U tends to infinity. Then Kennedy's result can be phrased as follows, with $n = 2$ and 3: for densities $1/(n+1) < \rho < 1/n$, the neutral ground state as $U \to \infty$ is a 'mixture' of C_n and C_{n+1}, in the sense that it is described by a sequence of occupied and vacant parallel lines of the slope shared by the lines defining C_n and C_{n+1}. It would be natural to conjecture that the statement holds for all n, but on the other hand, as Kennedy observed, configurations following this pattern are not the most homogeneous, which appears to contradict the predictions made on the basis of the effective interaction (section 2.2). Since the effective interaction takes account of only two-body terms, we expect it to be relevant at low (or high) density, and this suggests that Kennedy's rules break down at low (or high) density. We shall find (section 3.2) that this is precisely what occurs: the above statement is valid only for $n = 2$, 3 and 4. In particular, the characteristic configuration for density 1/6 does not follow the pattern.

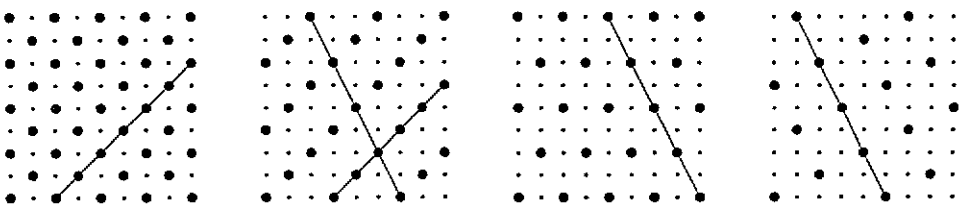

Figure 3. Characteristic configurations derived by Kennedy [17], which are neutral ground states for large U for the given densities. Large dots: occupied sites; small dots: vacant sites. The lines indicate the characteristic slopes discussed in the text.

2.4. Periodic ion configurations

Our numerical work is based on the construction of the *restricted* phase diagram, which means that we restrict the search for the lowest-energy state to periodic ion configurations with a unit cell having fewer than N_c sites, where N_c is a cut-off value depending on the available computer time. The reason for the restriction to periodic states is simply that this case is numerically tractable for motion in an infinite lattice. A similar approach has been very successful in the study of the one-dimensional Falicov–Kimball model [3, 9, 10], as well as other models with competing interactions [23].

The analysis of periodic configurations in two dimensions lacks the simplifying identities available in one dimension [24]. The key point is then the reduction of the model to a finite-dimensional eigenvalue problem, and the construction of the density of states, electron density and electronic energy as a function of electron chemical potential.

A two-dimensional periodic configuration is described by two primitive vectors a_1 and a_2, and the area of the unit cell is $N_0 = a_1 \times a_2$. If the electron wavefunction is ψ_r, as a function of lattice site r, Bloch's theorem states that under translation by a lattice vector $R = ma_1 + na_2$ with m and n integers, it satisfies

$$\psi_{r+R} = e^{ik\cdot R}\psi_r \tag{5}$$

where $k = (k_x, k_y)$ is the Bloch wavevector. The electron motion is thus reduced to a N_0-dimensional eigenvalue problem, whose eigenvalues we denote $E_{\nu k}$, with branch index $\nu = 1, 2, \ldots, N_0$. The wavevector k is restricted to a parallelogram-shaped Brillouin zone of area $(2\pi)^2/N_0$. All quantities of interest are calculated from the (normalized) density of states

$$Z(E) = \sum_{\nu} \int_{\mathrm{BZ}} \mathrm{d}k\, \delta(E - E_{\nu k}). \tag{6}$$

In particular, the electron density

$$\rho_e(\mu_e) = \int_{-\infty}^{\mu_e - U/2} Z(E)\, \mathrm{d}E \tag{7}$$

and total electronic energy per site

$$E_T(\mu_e) = \int_{-\infty}^{\mu_e - U/2} E Z(E)\, \mathrm{d}E \tag{8}$$

as a function of the Fermi energy (2). The energy per site in the grand canonical ensemble is defined as

$$E_{GC} = E_T - (\mu_e - U/2)\rho_e - (\mu_i - U/2)\rho_i. \tag{9}$$

These formulae are the basis of the numerical treatment in section 3.

The electronic spectrum is divided into N_0 branches. For the one-dimensional model, it can be shown [24] that the branches do not overlap and each forms a separate band, but in two dimensions this is not the case. It is easy to see, in fact, that the generic situation is that bands do overlap, and that many branches fuse into relatively few bands.

For some configurations, such as the chequerboard, the discrete eigenvalue problem is simple enough that some further progress can be made analytically [10, 14, 15]. An interesting class is the *stripe configurations*, which we define as those having (0, 1) or (1, 0) as primitive vectors. These have the appearance of vertical or horizontal stripes (see, for example, figure 9), and may be regarded as degenerate cases of Kennedy's characteristic configurations, with zero slope. The eigenvalue problem here reduces immediately to a one-dimensional one, and we find

$$Z(E) = (1/\pi) \int_{-2}^{2} Z_1(E + x)(4 - x^2)^{-1/2}\, \mathrm{d}x \tag{10}$$

where Z_1 is the density of states of the one-dimensional system obtained by taking a 'slice' perpendicular to the stripes. Z_1 consists of N_0 bands with inverse square root singularities at the edges. The two-dimensional density of states is obtained by a convolution with $(4 - x^2)^{-1/2}$, which eliminates most of the gaps.

The location of gaps in the electronic spectrum determines the transport properties of the corresponding state, and it is therefore informative to gain a qualitative understanding of the occurrence of gaps by considering the limiting cases of small and large U, for any periodic ion configuration. For small U we may treat the ion potential as a perturbation of the single $U = 0$ band, and then gaps do not open unless there is an electron density for which the Fermi surface is nesting, as at $\rho_e = 1/2$ in the chequerboard configuration. (The fact that nesting always occurs in one dimension is responsible for the opening of gaps in that case.) In fact, it is easy to see that the chequerboard structure is the only configuration which has precise nesting. With this one exception, therefore, there are no gaps for sufficiently small U.

For large U, gaps are expected, since at $U = \infty$ the electron states are localized. For $U > 8$, the principal gap is opened and has minimum extent $[4 - U, -4]$, but there are frequently other gaps as well, and these may be understood by large-U perturbation theory. The splitting of bands below the pricipal gap is given in first-order degenerate perturbation theory by the projection of the kinetic energy onto the degenerate subspace, which is an operator describing nearest-neighbour hopping restricted to the sublattice of occupied sites in the given configuration. If this sublattice permits no open orbits, forming a potential well which traps the electron, then the energy shifts are discrete and when broadened by higher-order perturbations form separate bands; we find then that the lower band is split into subbands. The number of subbands is at most equal to the number of full sites in the unit cell of the ion structure, but is sometimes fewer, when symmetry and higher-order splittings need to be taken into account. In contrast, if hopping on the full sublattice permits extended motion, the corresponding band is usually not split. Similarly, the splitting of bands above the principal gap is found by considering hopping on the empty sublattice.

As examples, we observe that the characteristic configurations in figure 3 have unbounded motion on the empty sublattice, and only one full site per unit cell, and therefore no splitting for large U; for small U there are no gaps. Therefore, we expect no gaps for any U, apart from the principal gap opening somewhere below $U = 8$. The same holds for the chequerboard structure, except that the principal gap opens at $U = 0$. Similarly the stripe configurations discussed above have no gaps other than the principal one. An example of a structure with other gaps is figure 15(a).

3. The restricted phase diagram

3.1. The computational method

Here we briefly describe the numerical procedure by which we have constructed the restricted phase diagrams in the grand canonical ensemble for a range of values of the interaction strength U.

The first step is to select a set of ion configurations to be taken into account. We have chosen to use the periodic configurations for which the (minimal) number of sites per unit cell, N_0, is less than or equal to a specified value, N_c.

The number of allowed configurations increases rapidly with N_c. In addition, the computer time required for diagonalization increases with N_0, so the total computer time increases very rapidly with N_c. The number of configurations can be reduced somewhat using the symmetry of the problem under rotation and reflection, and using the particle–hole symmetry, which implies that only configurations with an ion density less than 1/2 need be diagonalized. Nevertheless, the number of configurations approximately doubles with each unit increase in N_c. We have chosen $N_c = 15$, for which there are 10383 distinct allowed configurations.

It is not possible to enumerate here all the configurations in our trial set, and in fact it is not even possible to list all configurations that occur as ground states in our phase diagrams. Instead, in the following sections, we list a limited set of configurations occurring in the ground-state phase diagram which, we believe, illustrate the full range of behaviour of the model.

For each value of U and for each periodic configuration in our trial set, we have performed a numerical solution of the corresponding eigenvalue problem (see section 2.4). This involves finding the eigenvalues of an N_0-dimensional matrix for each value of k in a two-dimensional grid covering the Brillouin zone. The use of a grid of k-values amounts

to considering the electron motion in a finite lattice, and imposes a finite resolution on the resulting total energy. In order to minimize this source of numerical error, we have chosen a k-space grid which is not aligned with the Cartesian axes, to avoid clustering of eigenvalues due to symmetry of the grid, and we have employed an interpolation procedure in the calculation of integrated density of states and total energies from the eigenvalues.

Our calculations were performed with a k-space grid of 12 100 points for each configuration. By varying the resolution of the grid, we may estimate the resulting truncation error in the total energy calculation as less than 1 part in 10^4.

Finally, the phase diagram is constructed using the calculated total energies. For each value of the electron chemical potential μ_e, the electronic energy $E_T(\mu_e)$ determines the energy in the grand canonical ensemble, equation (9), for all values of ion chemical potential μ_i. This determines the range of μ_i, if any, in which the configuration has lower E_{GC} than any other considered so far. Repeating this calculation for all μ_e and all configurations in our trial set yields the restricted phase diagram, namely the ground-state ion configuration and electron density for each (μ_e, μ_i) point. The minimization of energy as a function of μ_i for fixed μ_e is aided by the fact that E_{GC} is a concave function of chemical potentials, which implies that the ground-state ion density is a nondecreasing function of μ_i for fixed μ_e [16].

3.2. Large U and neutral configurations

The phase diagrams for large U have a relatively simple structure, and so we begin our description of the numerical results by presenting, in figure 4, the restricted phase diagram for $U = 8$. With the one exception described below, the diagram for $U > 8$ is qualitatively the same as this one, and thus we expect $U = 8$ to be sufficiently large for the perturbation theory of [16, 17] to apply.

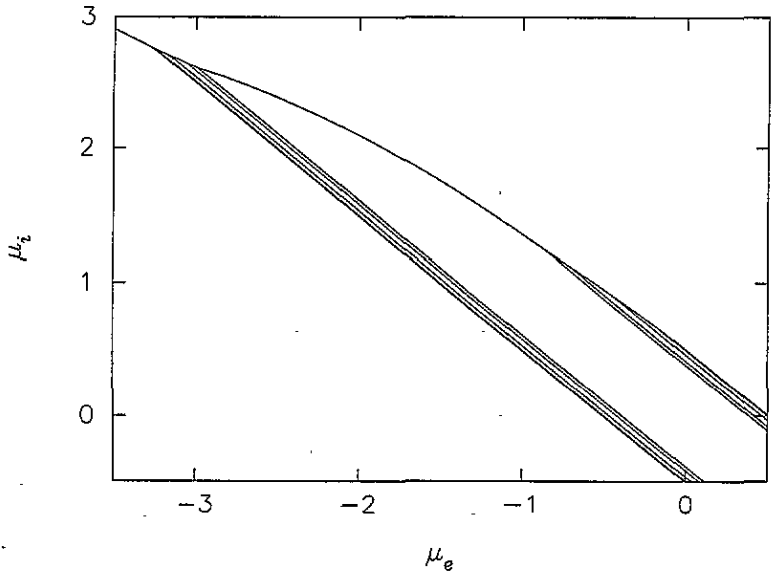

Figure 4. Calculated restricted phase diagram for $U = 8$. The upper and lower areas correspond to full and empty ground states, respectively. Various neutral ground states exist in the other domains, the largest (which includes the origin) corresponding to the chequerboard phase.

Only one quadrant of the plane of chemical potentials is represented, as the full diagram is symmetric about the origin, and the large domains occupied by full and empty phases need not be displayed. The diagram plots the phase boundaries which divide the plane of chemical potentials into domains, in each of which a single ion configuration is the ground state. The upper region corresponds to the full configuration, the lower region to the empty configuration, and the largest of the remaining regions is the chequerboard phase.

The phase diagram is fully consistent with the rigorous results (figure 2 and section 2.3): the plane is divided by a central portion into regions in which the full (+) and empty (−) configurations are ground states. For large U the exact results also guarantee the existence of a strip of μ_e in which all ground states satisfy the neutrality condition $\rho_e = \rho_i$. However the rigorous bound on the width of this strip vanishes for $U = 8$, and so the numerical results allow a stronger statement: for $U > 8$ all ground-state phases, apart from full and empty, are neutral, have E_F in the principal gap, and have phase boundaries which are diagonal straight lines.

The central portion is divided into diagonal stripes in which various periodic ion configurations are ground states, in a similar manner to the one-dimensional case. (Some of the stripes are too narrow to be clearly resolved.) The sequence of ion densities, reading from right to left at fixed μ_i, is 1/2, 4/9, 3/7, 5/12, 2/5, 1/3, 4/13, 3/10, 2/7, 1/4, 3/13, 2/9, 3/14, 1/5, 1/6, 1/8, 1/10, 1/11, 1/12, 1/14, the $\rho_i = 1/2$ phase being the large region containing the origin.

In section 2.3, we defined the characteristic configurations C_n as the $U \to \infty$ neutral ground states for densities equal to the reciprocal of an integer, and some of these may be obtained directly from our numerical data. For $\rho = 1/5$, 1/4, 1/3 and 1/2 they are in agreement with those derived rigorously by Kennedy [17], while for other densities they are the configurations depicted in figure 5. Most of the configurations given in the figure are present in the $U = 8$ phase diagram. The first exception is due to the fact that *the neutral ground state for density* 1/6 *changes with* U; this is a new feature of the two-dimensional model, since in one dimension the neutral ground states have never been observed to change with U. In the figure the ground states for $U = 8$ and $U = 20$ are given; the latter is then the characteristic configuration C_6. The second exception is that the density 1/15 configuration is taken from the $U = 7$ phase diagram, since it was not found for $U = 8$, perhaps because of the limited resolution.

Our numerical procedure does not, of course, determine the characteristic configurations rigorously, since there may be lower energy configurations of higher period. In addition, there are missing members of the series, notably those with density 1/7 and 1/9. It is likely that these phases would appear if the limit on unit cell area were increased, but our results to date leave certain characteristic configurations undetermined.

The characteristic configurations in figures 3 and 5 can be described as consisting of parallel lines of occupied or vacant sites. However, C_6 appears anomalous, as its structure has two ions per unit cell, and cannot be described by uniformly spaced lines of occupied sites. (It can be viewed as uniformly spaced half-occupied lines of slope 1.) Also, it does not share a slope with C_5, and therefore it does not appear possible to describe the $U \to \infty$ neutral ground states with $1/6 < \rho < 1/5$ in a similar way to Kennedy's [17] result for $1/4 < \rho < 1/2$. However, due to our limited set of trial configurations, we are not able to study the density range $1/6 < \rho < 1/5$: this question warrants further analytical study.

In the density range $1/5 < \rho < 1/2$, our results for densities intermediate between characteristic configurations are fully consistent with the 'conjecture' formulated in section 2.3: the ground-state configurations consist of parallel lines of occupied or vacant sites at a fixed slope. The configurations for $1/(n+1) < \rho < 1/n$ have the same

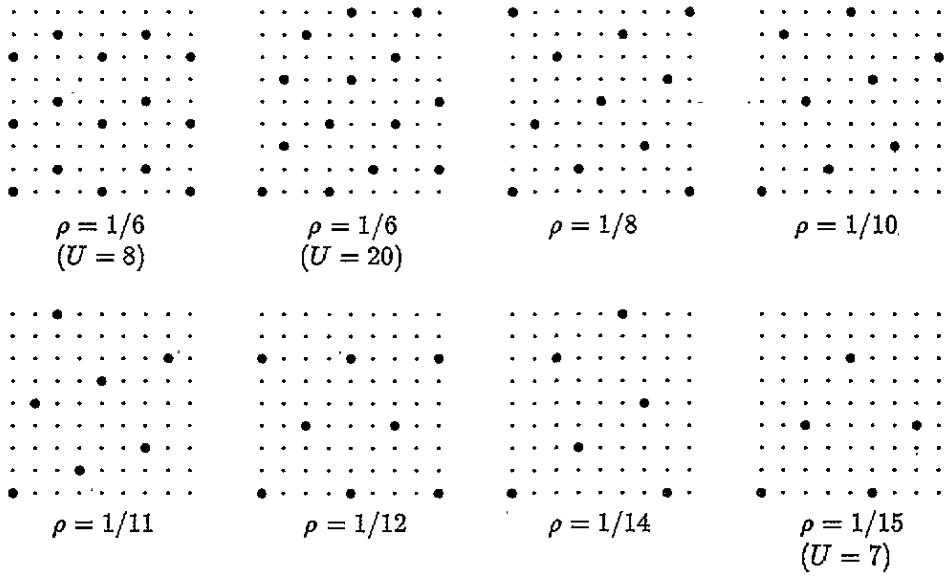

Figure 5. Neutral ground states for selected densities, taken from the $U = 8$ phase diagram unless otherwise indicated. Except for the first configuration, these are conjectured to be characteristic configurations, i.e. neutral ground states in the limit of large U with density equal to the reciprocal of an integer.

characteristic slope, which we denote s_n. Our numerical data yield $s_2 = 1$, $s_3 = 1/2$ and $s_4 = 1/2$, of which the first two agree with Kennedy's results [17].

In figure 6 we list the numerically determined ground states for the density range $1/3 < \rho < 1/2$, which are characterized by the slope $s_2 = 1/2$. The configurations are perfectly described by a surprisingly simple composition rule, with the structure of the Farey tree [9, 10]. Consider, for example, the density 2/5 state. In the Farey tree, 2/5 is a 'descendant' of 1/2 and 1/3, whose structures are given by the patterns (10) and (100), respectively, with slope 1. The pattern of the $\rho = 2/5$ ground state is (10100), which is simply the concatenation of the parent patterns. Similarly, the density 3/7 state (1010100) descends from 1/2 and 2/5, the density 4/9 state (10101010100) descends from 1/2 and 3/7, and the density 5/12 state (101010010100) descends from 3/7 and 2/5. This kind of hierarchical composition rule is typical of *one-dimensional* systems with competing interactions, such as the axial nearest-neighbour Ising model [25].

To summarize, we have found that the pattern established by Kennedy is obeyed for neutral phases in the density range $1/5 < \rho < 4/5$, and that all the ground-state ion configurations are described by a simple composition rule applied to the characteristic configurations. For densities outside this range, including the anomalous case $\rho = 1/6$, the pattern is not obeyed.

Let us now describe how this picture changes on reducing U. As already mentioned, the density-1/6 neutral configuration changes, as depicted in figure 5. Two further qualitative changes take place. Firstly, new families of ground states, not satisfying the neutrality condition $\rho_e = \rho_i$, begin to appear. Secondly, at rather low U, the neutral phases undergo a dramatic change. That is, although the existence of a region of neutral phases, with Fermi energy in the principal gap, persists to small U, the corresponding ion configurations no longer have the structure described above, and all the characteristic configurations disappear,

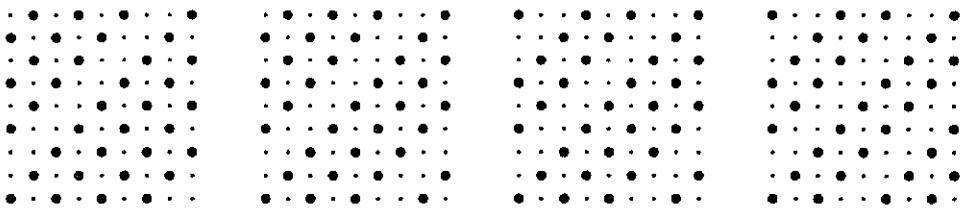

Figure 6. Neutral phases with $1/3 < \rho < 1/2$ in the $U = 8$ restricted phase diagram.

except for the chequerboard. For example, in the $U = 1$ phase diagram we observe a sequence of neutral phases with ion densities 1/2, 7/15, 3/7, 5/12, 2/5, 3/8, 5/14, 1/3; four of them are pictured in figure 7. Here, the ions adopt arrangements constructed by introducing homogeneously spaced lines of vacancies, aligned with the lattice axes, into the chequerboard structure. Configurations in this family have a principal gap even at rather low U, and when they are ground states have E_F in the gap. Once again, the ground states are regular and essentially one-dimensional in character.

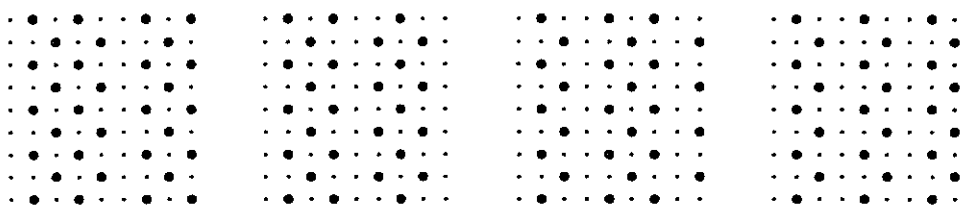

Figure 7. The sequence of neutral ground states in the $U = 1$ restricted phase diagram.

3.3. Stripe configurations

Figure 8 shows an enlargement of a region of the restricted phase diagram for $U = 6$, at the tip of the domain of neutral phases. (The remaining phase diagram is similar to the $U = 8$ case.) There appear two features not present at $U = 8$. One is a new phase adjoining the (+) region, marked B in the figure, which will be described in section 3.5 below. The second is an entire family of new phases at A, adjacent to the neutral region and the segregated phase.

This new family consists of stripe phases, which were defined in section 2.4 as those with a one-dimensional unit cell, with unit period along the perpendicular direction. The ion densities of the stripe phases in region A of figure 8, reading from right to left, are 1/3, 4/13, 3/10, 2/7, 3/11, 4/15, 1/4, 3/13, 2/9, 3/14, 1/5, 2/11, 1/6, 2/13, 1/7, 2/15, 1/8 and 1/9. This sequence contains all fractions in the range [1/9, 1/3] with denominator less than or equal to 15, in decreasing order. The configurations themselves also obey a regular hierarchy, as illustrated in figure 9, which lists the ground-state stripe configurations with ion densities 1/3, 2/7 and 1/4. Once again, the structure is that of the Farey tree: the density-1/3 and density-1/4 states are described as (100) and (1000), respectively, and their 'descendant' state of density 2/7 has the concatenated structure (1001000). The descendant of 1/3 and 2/7 has the structure (1001001000) with density 3/10, and so on.

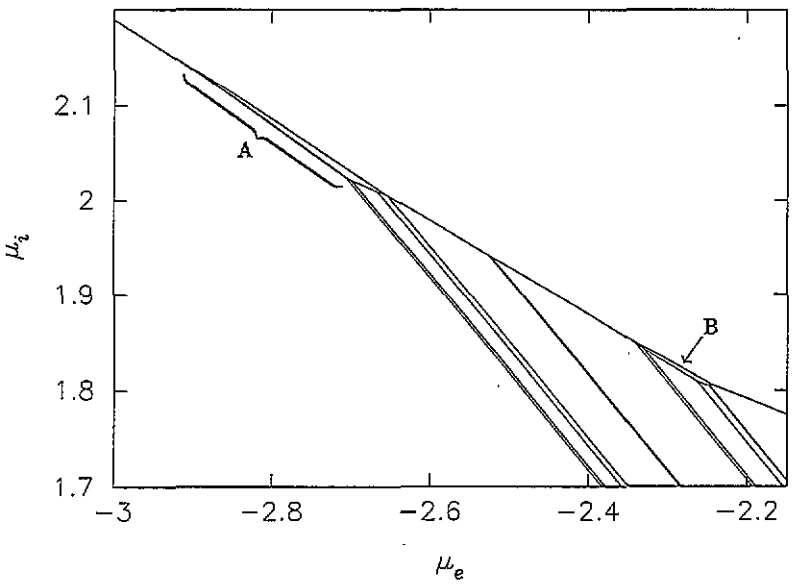

Figure 8. Detail of the calculated restricted phase diagram for $U = 6$. Domains labelled A correspond to the stripe configurations (section 3.3), and B points to an unusual insulating phase discussed in section 3.5.

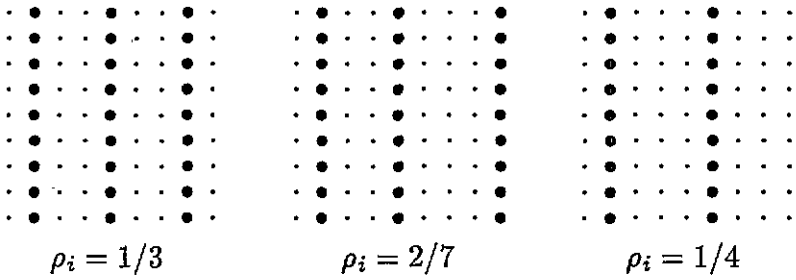

Figure 9. The ground-state stripe configurations with ion densities 1/3, 2/7 and 1/4 from the $U = 6$ restricted phase diagram.

In all the restricted phase diagrams we have constructed for $U \leqslant 6$, namely $U = 6$, 4, 2 and 1, we have found a region in which stripe configurations are the ground states. Invariably, the sequence of phases is that of the Farey tree with the simple composition rule. However, they differ in the range of densities which is represented; for example for $U = 2$ only densities in the range $[1/4, 1/2]$ are found in the stripe region, and for $U = 1$ only $[1/3, 1/2]$. Thus, extrapolating to arbitrarily high period, we may conjecture that the sequence of stripe phases forms a devil's staircase, but that the staircase is not complete, since a limited range of densities appears. This incompleteness, especially for low U, occurs also in the one-dimensional model for the neutral phases [9, 10].

A very surprising feature of the stripe configurations in the phase diagram is that the boundaries between them are very nearly parallel. This is also a feature of the phase diagram of the one-dimensional model, where it is due to the fact that the Fermi energy lies in a gap of the single-electron density of states, and hence the phase boundaries are straight lines of the same slope. Here, however, the explanation must be different, since

the phase boundaries are *curved*, but appear to be parallel nevertheless. Furthermore, the stripe configurations have no gaps in the range of U under consideration (as expected from the qualitative arguments of section 2.4). Instead, it happens that the density of states is such that the ratio of electron to ion density is very nearly independent of the configuration (although dependent on electron chemical potential), so that all the phase boundaries at fixed μ_e have the same slope.

3.4. Molecules, and multiple and staggered stripes

In figure 10 we present a detail of the calculated phase diagram for $U = 2$. Although we expect the diagram to be accurate in that the precision of our calculation is sufficient to resolve energy differences between configurations, it is likely that for this low U there are inaccuracies due to the limit on the period of the trial configurations. In other words, we do not expect the restricted phase diagram to represent fully the true phase diagram. Nevertheless, we may identify some regular families of ground states: in the lower part of the figure, we have the neutral phases discussed in section 3.2, the intermediate shading corresponds to stripe configurations (section 3.3), the light shading corresponds to staggered stripes (see below), and in the dark shaded area we find molecule formation. Other unshaded areas do not fit into one of these categories, and may correspond to genuine ground states (section 3.5) or to artefacts of the finite set of trial configurations.

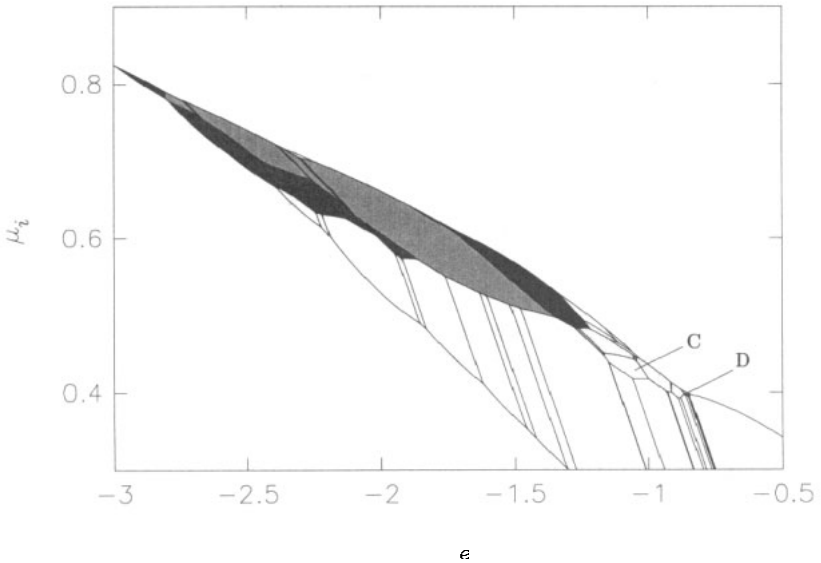

Figure 10. Detail of the restricted phase diagram for $U = 2$. Light shading: staggered stripe phases; medium shading: stripe phases; heavy shading: molecular lattices. Phases labelled C and D are discussed in section 3.5.

The heavily shaded area in figure 10 contains a variety of configurations consisting of molecules. Some examples are listed in figure 11: these occur with increasing $|\mu_e|$ in the phase diagram. In (a) to (c) we observe the formation of dimers, which then repel each other resulting in dimer lattices with various orientations, or in mixed lattices of dimers and single ions. Figure 11(d) demonstrates the formation of a lattice of molecules of four ions. There exist also ground states consisting of linear molecules of three or more ions. Similar

types of molecule configurations are grouped together in the phase diagram. In figure 10, the molecular phases lying below the staggered stripe domain are various lattices of dimers, the phase in the extreme tip is the four-ion molecule of figure 11(*d*), and the molecular phases lying furthest to the right and adjacent to the full configuration involve molecules of vacancies.

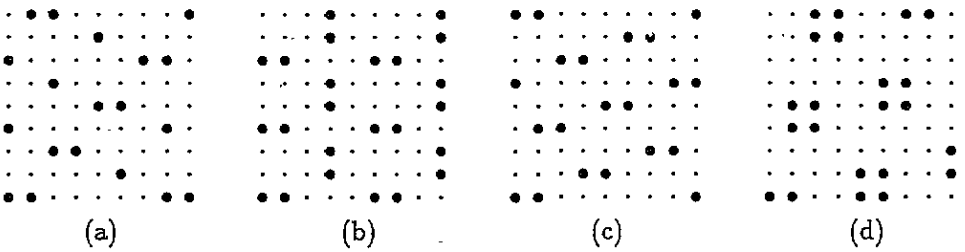

Figure 11. Selected molecular lattices occurring in the $U = 2$ phase diagram.

For many of these molecular configurations the density of states has a gap, and the Fermi energy lies in a gap when the configuration is the ground state. However, this gap is not the principal gap, and the resulting phase is not neutral: instead, invariably, the electron density is very close to one electron per molecule. (This phenomenon has been observed previously in the one-dimensional FKM [10].) There appears to be some regularity in the structure of this family of ground states, but our resolution is not sufficient to explore this in detail.

When U is reduced further to 1, the restricted phase diagram appears as in figure 12. Here, the problems associated with finiteness of the set of trial configurations is most serious, but it is possible to make some general statements. The various families of ground states indicated in the $U = 2$ phase diagram (figure 10) also appear here, with the staggered stripe configurations (described below) particularly prominent. An additional family occurs in the extreme tip of the nontrivial portion of the diagram, between molecular lattices and the segregated phase. This is the family of multiple-stripe configurations, illustrated in figure 13. These patterns resemble the molecular lattices of the one-dimensional model [10]: lines of ions in a stripe configuration attract each other, forming stripe pairs which subsequently repel, resulting in a regular array of pairs. As with other stripe phases, these do not have gaps in their single-electron densities of state.

The regions indicated by light shading in figures 10 and 12 contain a further regular family of configurations, which we term staggered stripes. A part of the full sequence occurring for $U = 1$ with increasing μ_e is given in figure 14. All the configurations have ion density 1/2, and the sequence begins with the $\rho_i = 1/2$ stripe configuration and ends with the chequerboard, the intermediate phases being, in a sense, interpolations between the two structures. In other words, as μ_e is increased from the stripe phase, increasing numbers of regularly spaced faults appear in the stripes, until the chequerboard is gradually reached. Thus, with changing μ_e, the system undergoes a (presumably infinite) sequence of transitions between configurations of the same ion density. Another interesting property of this family is that for low $|\mu_e|$ ('nearly chequerboard' configurations) the Fermi energy lies in a gap and the dependence of electron density on μ_e forms a devil's staircase, while for larger $|\mu_e|$ the configurations no longer have gaps and the staircase becomes smeared out.

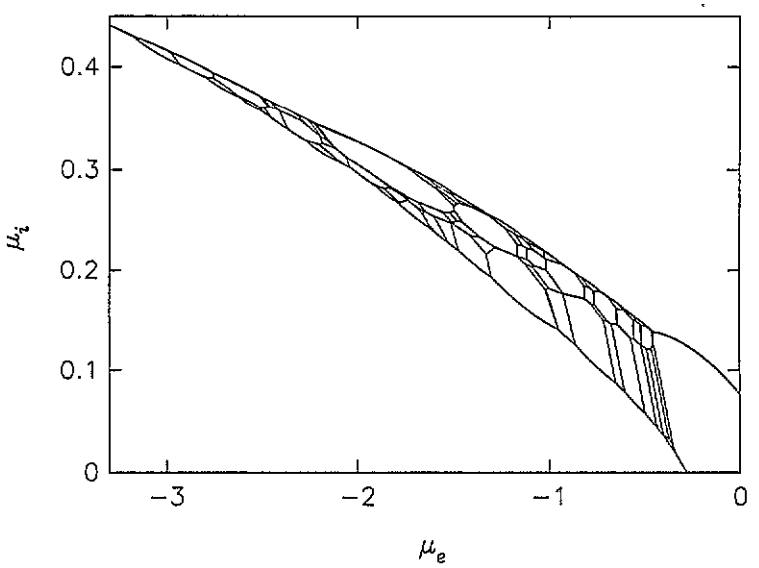

Figure 12. Calculated restricted phase diagram for $U = 1$. The shaded areas correspond to the staggered stripe phases (section 3.4).

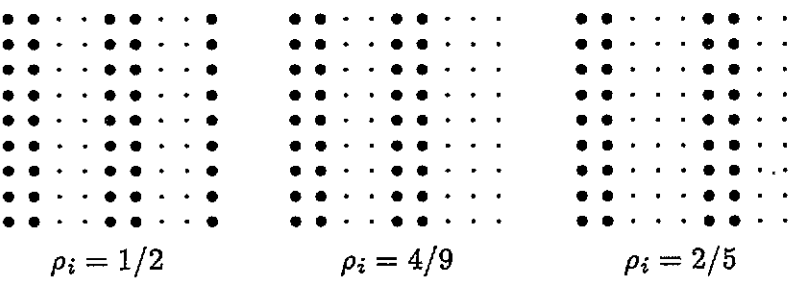

Figure 13. Selected multiple-stripe configurations occurring in the $U = 1$ phase diagram.

3.5. Other configurations

There are a number of configurations appearing as ground states in the restricted phase diagrams, particularly for low values of U, which do not fall into any of the above families. It is not practical to list all of them; rather, we wish to mention only one class of configurations which seem important simply because they do not seem to fall into readily identifiable families, and do not have any of the one-dimensional properties characteristic of the families considered previously. In other words, we describe configurations which have an essentially two-dimensional character.

Several examples are given in figure 15. Configuration (*a*) appears in the phase diagram for intermediate U, and its ion–vacancy inverse is the phase marked B in figure 8. Although this could be considered a lattice of dimers, it does not occur adjacent to other dimer configurations, and in fact it appears at much larger U than any other dimer states. Therefore, we view it as forming a class of its own. Finally, we mention the configurations of figure 15, (*b*) and (*c*), which occur in regions marked C and D, respectively, in the $U = 2$ phase diagram (figure 10).

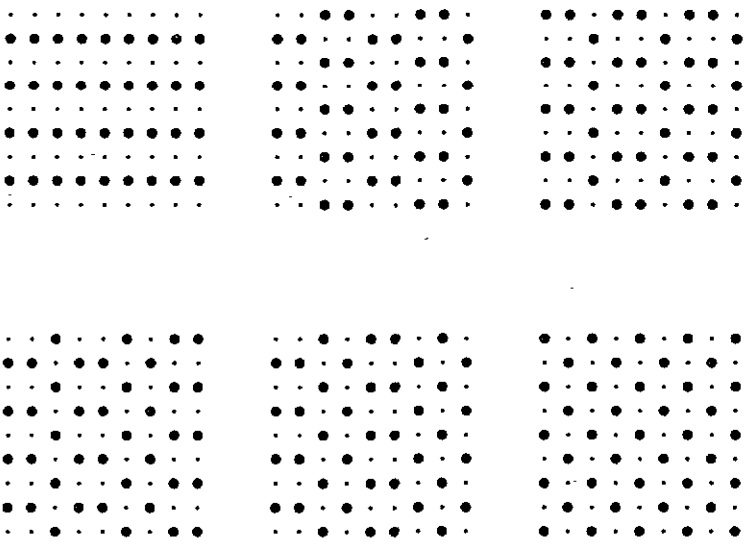

Figure 14. Selected staggered stripe configurations occurring in the $U = 1$ phase diagram, given in left to right order in figure 12.

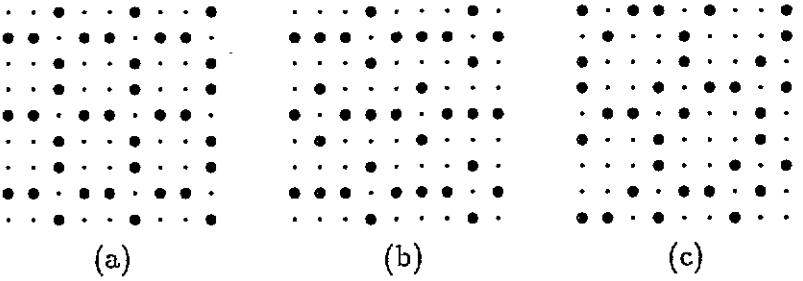

Figure 15. Miscellaneous configurations occurring in the restricted phase diagrams: (*a*) for $U = 6$; (*b*) and (*c*) for $U = 2$.

4. Discussion

Let us briefly summarize the changes that occur as the interaction constant U is varied. As in the one-dimensional case, and in accordance with the general discussion of section 2.2, the phase diagram becomes increasingly complicated as U decreases. For large U, the only phases appearing (as finite regions) are neutral ones ($\rho_e = \rho_i$) and the full and empty configurations. All the neutral phases are insulating. For densities in the range $1/5 < \rho < 4/5$, they have ion configurations obeying a simple set of rules (section 3.2). Outside this range their structure has yet to be completely characterized, but consideration of the effective two-body ion interactions (section 2.2) suggests that the ground states for low or high density are homogeneous in the distribution of ions. When U is decreased to about 6, the stripe configurations (section 3.3) begin to appear, and these obey a composition rule identical to that observed in the one-dimensional model. At the same time, the first of a class of configurations which must be considered essentially two-dimensional (section 3.5) appears. On decreasing U further, we observe new families of ground-state configurations, the molecular lattices, multiple stripes and staggered stripes (section 3.4).

The Falicov–Kimball model is formally equivalent to an Ising model with a highly complicated and frustrated effective interaction, and indeed the various families of ground-state configurations discussed here are reminiscent of ground states found for certain frustrated Ising models on two-dimensional lattices [26].

There are many similarities in behaviour between the Falicov–Kimball models in one and two dimensions. Some of them are quite general, and independent of dimension, as has already been established by Gruber *et al* [16]. Our work has identified other features common to both one-dimensional and two-dimensional cases.

(i) The only ground-state phases for large U which are not translationally invariant are the neutral ones. All neutral phases which appear on the ground-state phase diagram are insulating (with the Fermi level in a gap). As a consequence, the boundaries between different neutral phases are straight line segments with unit slope.

(ii) Configurations of the ions corresponding to the main families of ground-state phases are described by a simple composition rule, with the structure of the Farey tree.

(iii) There is a critical value of $U = U_c$, such that for $U < U_c$ there is an interval of ionic densities, $(\tilde{\rho}_i(\mathrm{U}), 1-\tilde{\rho}_i(\mathrm{U}))$, with $\tilde{\rho}_i(\mathrm{U}) > 0$, to which the neutral phases are confined.

(iv) The formation of molecules takes place for small enough values of U.

(v) The effective potential between two ions in the neutral case is purely repulsive for large U, while for intermediate and small U it is attractive at short range and repulsive at long range.

There are, however, important differences between the one-dimensional and two-dimensional phase diagrams. In particular, we find that in the two-dimensional case.

(i) The neutral phases, for at least a range of densities, do not correspond to the most homogeneous distributions of the ions over the lattice, as already proven by Kennedy [17] for some cases.

(ii) The distribution of the ions for some neutral phases changes with U. This phenomenon was not observed in the one-dimensional model, where the ground-state neutral configuration for a given ρ_i persists for all values of U. In two dimensions it appears in two ways. Firstly, for density $1/6$ there is a transition between two different ion configurations at fairly large U. Secondly, for smaller U the sequence of neutral phases changes completely, with only a set of chequerboard-like configurations remaining (section 3.2 and figure 7).

(iii) In one dimension, any periodic ion configuration has an electronic spectrum split into as many bands as the number of sites in the period. With the exception of full and empty phases, all phases found as ground states are insulating, and all the phase boundaries are straight line segments. In two dimensions, however, many non-neutral ground-state phases which appear on the phase diagram for intermediate and small U are conducting, and in fact have no gaps at all in their energy spectrum. Consequently the boundaries between these phases are not straight line segments. Surprisingly, however, the boundaries are nearly parallel for the family of stripe configurations (see section 3.3).

For the one-dimensional model, an explanation for the composition rule which describes the construction of ground-state phases for small U [3] involves the stabilization effect of the gap created at the Fermi level when the ions adopt a suitable periodic arrangement. The most stable configuration is that with the largest gap. (For large U, the same rule can be justified on the basis of an effective ion interaction which is repulsive and convex [27].) In its simplest form, this argument is restricted to one dimension, since in that case the Fermi surface consists of two points and always has perfect nesting. The striking property of the two-dimensional model that several families of phases are described by a form of

one-dimensional composition rule, even when there are no gaps, must then be related to partial nesting of the Fermi surface. In other words, a periodic ion arrangement is stabilized by the opening of a gap over part, but not all, of the Brillouin zone.

We now turn to the question of segregation. In the terminology of section 2.3, we have found that the boundary between the full and empty phases *does* continue inside the domain $\tilde{\mathcal{D}}$, and therefore that there are a range of densities for which the ground state is the segregated phase. This is a (phase-separated) mixture of the full configuration containing all the electrons, and the vacuum (the empty phase without electrons). The same feature has been proved rigorously in one dimension [11, 28] and in infinite dimensions [19]; our work supports the conjecture that it occurs for any dimension. A complication of models in more than one dimension is that one can imagine the segregated phase with various shapes of boundaries between the full configuration and the vacuum. It would be interesting to study the optimal shape of the boundary for a given ρ_i and ρ_e.

The phase diagram in the canonical ensemble (ρ_e–ρ_i plane) for large U is dominated by segregated and neutral phases, in both one and two dimensions, in the sense that 'most' of the phase diagram corresponds to a segregated ground state, a sequence of special phases occurs on the neutral line $\rho_e = \rho_i$, and the remaining region (containing mixtures between neutral phases and mixtures of neutral phases with full or empty configurations) shrinks to zero in area as U tends to infinity. The detailed comparison of canonical phase diagrams for the full range of U can in principle be carried out using our results, but it is not trivial to transform from one representation to the other, and we leave this topic for a future publication.

Acknowledgments

We thank Martin Long for helpful discussions. GIW is grateful to the Institute for Low Temperature and Structure Research, Polish Academy of Sciences, Wrocław, for hosting a visit and to the Committee for Scientific Research (Poland) for funding it. RL acknowledges the financial support of the Committee for Scientific Research (Poland) under grant number 2P30214704 and of a Research Fellowship from the Commission for the European Community and is grateful to Professor S W Lovesey and the Rutherford Appleton Laboratory for hospitality during an extended visit.

References

[1] Falicov L M and Kimball J C 1969 *Phys. Rev. Lett.* **22** 997
[2] Kennedy T and Lieb E H 1986 *Physica* A **138**
Lieb E H 1986 *Physica* A **140** 240
[3] Freericks J K and Falicov L M 1990 *Phys. Rev.* B **41** 2163
[4] Janiš V and Vollhardt D 1993 *Z. Phys.* B **91** 317; 1993 *Z. Phys.* **91** 325
[5] Si Q, Kotliar G and Georges A 1992 *Phys. Rev.* B **46** 1261
[6] Freericks J K, Jarrell M and Scalapino D J 1993 *Phys. Rev.* B **48** 6302
[7] Łyżwa R and Domański Z 1994 *Phys. Rev.* B **50** 11381
[8] Freericks J K 1993 *Phys. Rev.* B **47** 9263
[9] Lach J, Łyżwa R and Jędrzejewski J 1993 *Acta Phys. Pol.* A **84** 327; 1993 *Phys. Rev.* B **48** 10783
[10] Gruber C, Ueltschi D and Jędrzejewski J 1994 *J. Stat. Phys* **76** 125
[11] Lemberger P 1992 *J. Phys. A: Math. Gen.* **25** 715
[12] Gruber C, Lebowitz J L and Macris N 1993 *Europhys. Lett.* **21** 389; 1993 *Phys. Rev.* B **48** 4312
[13] Brandt U and Schmidt R 1986 *Z. Phys.* B **63** 45; 1987 **67** 43
[14] Jędrzejewski J, Lach J and Łyżwa R 1989 *Phys. Lett.* A **134** 319; 1989 *Physica* A **154** 529
[15] Gruber C, Iwanski J, Jędrzejewski J and Lemberger P 1990 *Phys. Rev.* B **41** 2198

[16] Gruber C, Jędrzejewski J and Lemberger P 1992 *J. Stat. Phys.* **66** 913
[17] Kennedy T 1994 *Rev. Math. Phys.* **6** 901
[18] Freericks J K 1993 *Phys. Rev.* B **48** 14797
[19] Brandt U and Mielsch C 1989 *Z. Phys.* B **75** 365; 1990 *Z. Phys.* B **79** 295; 1991 *Z. Phys.* B **82** 37
[20] Stoneham A M 1985 *Theory of Defects in Solids* (Oxford: Clarendon) ch 5
[21] Bursill R J 1994 *Physica* A **206** 521
[22] Barma M and Subrahmanyam V 1989 *Phase. Trans.* **16/17** 303
[23] See, for example, Bak P 1982 *Rep. Prog. Phys.* **45** 587
Heine V 1987 *Competing Interactions and Microstructures: Statics and Dynamics* ed R LeSar, A Bishop and R Heffner (Berlin: Springer) p 2
[24] Lovesey S W, Watson G I and Westhead D R 1991 *Int. J. Mod. Phys.* B **5** 1313
Łyżwa R 1992 *Phys. Lett.* A **164** 323; 1993 *Physica* A **192** 231
[25] Yeomans J 1988 *Solid State Physics* vol 41, ed H Ehrenreich and D Turnbull (San Diego, CA: Academic) p 151
[26] Brandt U 1983 *Z. Phys.* B **53** 283
Brandt U and Stolze J 1986 *Z. Phys.* B **64** 481
[27] Hubbard J 1978 *Phys. Rev.* B **17** 494
Bak P and Bruinsmaa R 1982 *Phys. Rev. Lett.* **49** 249
Aubry S 1983 *J. Phys. C: Solid State Phys.* **16** 2497
[28] Brandt U 1991 *J. Low Temp. Phys* **84** 477